ARTICLE TEMPLATE

Molecular Simulation of Hydrogen Storage and Transport in Cellulose

M.R. Stalker[a,b], J. Grant[b,c], C.W. Yong[d], L.A. Ohene-Yeboah[a,b], T.J. Mays[e] and S.C. Parker[b*]

[a]Centre for Sustainable Chemical Technologies, University of Bath, Bath BA2 7AY, United Kingdom;
[b]Department of Chemistry, University of Bath, Bath BA2 7AY, United Kingdom;
[c]Computing Services, University of Bath, Bath BA2 7AY, United Kingdom;
[d]Scientific Computing Department, STFC Daresbury Laboratory, Daresbury WA4 4AD, United Kingdom;
[e]Department of Chemical Engineering, University of Bath, Bath BA2 7AY, United Kingdom

ARTICLE HISTORY
Compiled April 17, 2019

ABSTRACT
In this work we describe a computational workflow to model the sorption and transport of molecular hydrogen in cellulose frameworks. The work demonstrates the value of the molecular dynamics code, DL_POLY and Monte Carlo code, DL_MONTE sharing common input formats to enhance the compatibility of the codes, being supported by DL_FIELD. Structures generated using cellulose-builder were processed by DL_FIELD to generate input files for DL_POLY using the OPLS_2005 force field. After relaxation in molecular dynamics, structures were used for GCMC simulations in DL_MONTE before passing back to DL_POLY to evaluate transport properties at different levels of sorption. While no hydrogen sorption was seen in pure crystalline cellulose, increasing separation between layers did allow sorption. When slit-pores were sufficiently wide, interactions with the cellulose led to the volumetric density of adsorbed hydrogen exceeding vacuum density at accessible partial pressures as well as allowing diffusion through the system. These model systems can give useful insight into the behaviour of amorphous cellulose in future simulation and experiment.

KEYWORDS
molecular modelling; molecular dynamics (MD); Monte Carlo (MC); cellulose; hydrogen storage

1. Introduction

Current global energy demands rely upon fossil fuels and their environmental impacts. With fossil fuel reserves depleting and global energy demands increasing, the need for more sustainable fuel sources is increasingly recognised. As a result, there is growing interest in the development of alternative, renewable energy sources and energy storage.[1]

Hydrogen is a renewable and clean burning fuel which can provide on-demand power, making it a strong candidate to become an integral part of the future en-

*Corresponding author. Email: S.C.Parker@bath.ac.uk.

ergy landscape.[2–5] The process of using hydrogen as an energy vector is made up of three distinct parts, namely: production, storage and utilisation. The storage of hydrogen is regarded as the most challenging aspect of integrating hydrogen into the energy mix, due to the low volumetric density of hydrogen gas. [6]

Methods used to store hydrogen can be broadly divided into two categories: chemical storage and physical storage (including sorption). [4] Chemical storage is the inclusion of hydrogen (hydrogenation) in chemical compounds. At high temperatures hydrogen can then be liberated (dehydrogenation) from the compounds. Typical chemical hydrogen storage compounds range from light metal hydrides to complex hydrides.[3,7–9]

Physical storage can be enhanced through sorption processes. Sorption of hydrogen relies upon favourable interaction energies between molecular hydrogen and porous materials. The high surface area of porous materials increases the number of interactions between the storage material and hydrogen. The extent of hydrogen storage depends upon the specific surface area and pore sizes within the storage material as well as the strength of the interactions.[3] Despite being numerous, the interactions are weak (typically $<$10 kJ mol^{-1}) and as a result, adequate storage relies upon low temperatures and high pressures.[7] Candidates for hydrogen storage materials are typically crystalline, including carbonaceous structures, intrinsically porous frameworks such as metal-organic frameworks (MOFs), covalent organic frameworks (COFs) and zeolites. [3,4,7,10–12]

In addition to crystalline materials, recent research has investigated the use of porous polymers for hydrogen storage. Porous polymers provide a lightweight alternative to traditional metal-based adsorbents, [5,11,13,14] since they pack in a way that results in large voids, which also allows absorptive molecules to permeate their structures. [15] Polymers of intrinsic microporosity (PIMs), and hyper-cross linked polymers (HCPs) are porous polymers which have been considered for hydrogen storage,[4–6,16] but the distributions of pore sizes and structures complicates analysis. As a result, a number of researchers have applied computational analysis to study the properties of PIM. [14,17–20] and HCP [15,21,22] structures.

Cellulose is the most abundant organic polymer in the biosphere, with over 100 billion metric tons being synthesised annually while its biodegradability makes it more sustainable than conventional polymers.[23–27] The polymer is primarily synthesised within plant cell walls, where it serves as the principal structural polymer forming characteristic hierarchal structures embedded within a matrix of complex polysaccharides, including amorphous cellulose.[28–30]

Individual chains of cellulose comprise β-(1,4) glycosidic linkages of glucose residues which assemble into sheet structures, driven by intermolecular hydrogen bonds, which further assemble into 3-dimensional structures due to van der Waals interactions.[27, 29–34] The resultant crystalline structures are referred to as microfibrils, and exist as a mixture of two allomorphs, Iα and Iβ. [27,32,34,35] Cellulose displays much greater chemical and structural complexity than conventional polymers and is also insoluble in traditional solvents, making experimental studies of cellulose challenging. As a result of such experimental complexities, the simulation of cellulose has been pursued widely in the literature.

Carbohydrates such as cellulose demonstrate a high density of chemical functionality and have a number of possible configurations making their structures complex to simulate. Classical modeling has typically been used, but the force field influences the outcome of classical simulations.[36–39] As a result, a range of biomolecule-specific families of force fields such as CHARMM [40], AMBER[41], and OPLS[42] have been developed to model molecules such as carbohydrates.

Molecular modeling has been applied to understand structural properties including the crystalline networks [43,44], mechanical properties [45–48] and thermal transitions [49–52] of cellulose. Simulations have also been used to investigate the interactions between cellulose structures and a range of small molecules including solvents [45,53–55] and model aromatic compounds [56–59].

As a result, molecular modeling provides a route to evaluate the feasibility of cellulose as a candidate for hydrogen storage, however, to our knowledge, no research has previously been reported. In this article we describe the methods we have used to study the sorption and transport of hydrogen molecules in various cellulose structures, before discussing our findings and their implications for cellulose as a candidate for hydrogen storage.

2. Methods

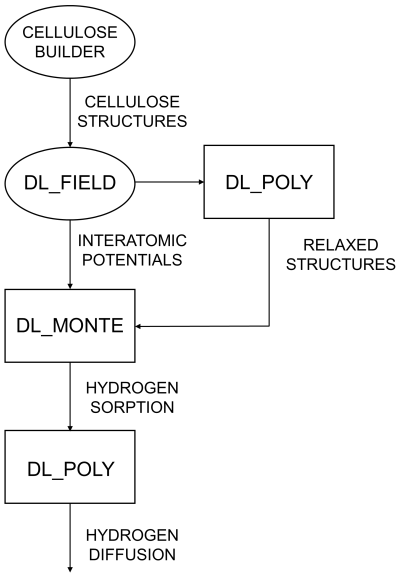

Figure 1. Workflow demonstrating the method developed for modeling cellulose. Structural analysis and production steps are represented by an oval and simulation steps are represented by a rectangle.

This research follows the workflow summarised in Fig. 1 and makes use of the compatability between DL_POLY [60,61] and DL_MONTE [62,63]. This uses DL_POLY for molecular dynamics to relax structures and study transport properties while using the increased range of ensembles open to Monte Carlo DL_MONTE e.g. for sorption. This approach ensures that each stage of the calculation is able to make use of the most efficient method for that problem. DL_FIELD [64] was used to generate specific force fields for the systems of interest while the initial configurations were generated using cellulose-builder[65].

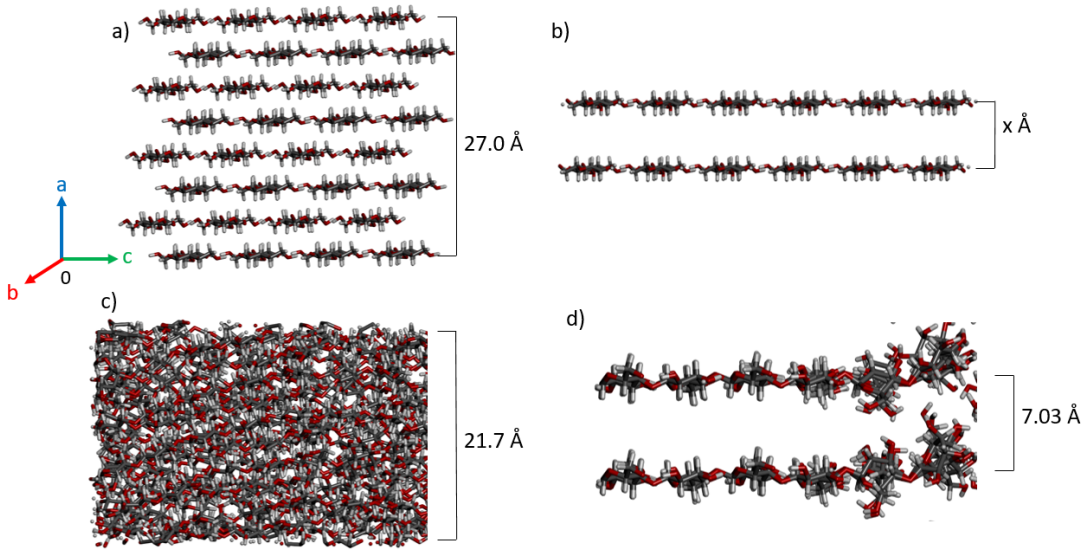

Figure 2. a) micro-fibril and b) slit pore cellulose structures (where $x = 4.76, 5.76, 6.76, 7.76$Å) were generated directly from cellulose-builder . c) Amorphous and d) partially pinned structures (showing initial $x = 7.76$Å) structures were prepared by relaxing in DL_POLY.

2.1. Structure Generation

Cellulose-builder is an open-access script developed by Gomes and Skaf [65]. The script generates configurations in *xyz* or *pdb* format based on the crystallographic data from Nishiyama et al. [34,66]. The script is capable of generating the native Iα and Iβ allomorphs, the II and III polymorphs which are found in solvated systems, and can control the degree of polymerisation (DP). The crystalline structures were generated directly from cellulose-builder and are shown in Fig. 2a. These configurations comprised eight alternating layers of four origin and centre chains of two, four, six, eight and twelve repeat units in length (DP = 2,4,6,8,12) were built using the `fibril` command with periodic boundary conditions in all directions. For the shorter chains (DP = 2,4) the systems were also grown to comprise three and two units respectively so that the system size was large enough for the cut-off length and periodic boundary conditions.

Processing conditions such as drying and solvent exchange have been demonstrated to influence the pore characteristics of cellulose structures. [67,68] In order to investigate the effect of pore size on the hydrogen storage capability of cellulose structures, slit pore structures with incremental pore sizes were produced. The `center` command was used to generate a monolayer of cellulose Iβ centre chains comprised of six cellulose chains, six repeat units (DP = 6) in length. The monolayers were then grown with a modified a lattice vector to achieve structures with different inter-layer separations as indicated in Fig. 2b. The system sizes used resulted from increasing the distance between layers by increments of 1 Å. The configurations also served as the starting point for generating amorphous and pinned models of cellulose as described in Section 2.3.

2.2. DL_FIELD Processing

DL_FIELD was used to identify molecules and assign atom types in order to produce input files for DL_POLY . The atom types were assigned the OPLS_2005 parameter set, as the force field has been specifically optimised for carbohydrate systems such as cellulose.[37,64,69,70] The complexity of carbohydrates and cellulose in particular required additional functionality to be developed for DL_FIELD as well as the inclusion of the force field definitions. Provided the system configurations that contained pyranose sugar units are in the stable 'chair' conformations, DL_FIELD can distinguish various pyranose isomers, as well as their corresponding anomeric structures. Such detection processes are based on a series of geometrical analysis to determine the relative orientations of the hydroxyl groups contained in the sugar units. This functionality is available in DL_FIELD version 4.2 onwards, which was first released in January 2018.

2.3. Structural Relaxation

It was necessary to run initial molecular dynamics calculations to crystalline structures using DL_POLY to validate the creation of the configurations and assignment of the force field. These calculations were performed according to the protocols 1 and 2 given in Table 1, for the full range of DP generated using cellulose-builder. Protocol 1 allowed for controlled relaxation of the end groups, which are close in crystal structures and protocol 2 allowed relaxation at constant pressure to validate behaviour. Once the accuracy of the structures and force field generation had been validated, further simulations were used to generate initial configurations for gas sorption studies in partially relaxed and amorphous structures.

Table 1. Molecular dynamics simulation conditions of simulation protocols used in this work.

Protocol	1	2	3	4
Ensemble	NVT	NST	NpT	NVT
Temperature (K)	298	298	298	298
Pressure (bar)	-	1	1	-
Length (ps)	5	1000	1000	1000
Step length (fs)	1	1	1	1
Thermostat	Nosé-Hoover			
Cut Off Distance (Å)	10			

Natural crystalline cellulose exists within a matrix containing amorphous cellulose chains. To simulate amorphous cellulose chains, shown in Fig. 2c crystalline structures of cellulose polymers (DP = 6) were relaxed using initial short simulations, protocol 1. Annealing simulations were then performed using protocol 3, allowing the structures and simulation cells to relax.

Traditional hydrogen storage materials such as MOFs and zeolites, contain ordered porous regions. To mimic the ordered pore structure of these slit pore materials, crystalline structures of cellulose polymers DP = 6 were relaxed whilst pinning linking glycosidic oxygens to produce pinned structures, shown in Fig. 2d. The pinned structures were subjected to initial short simulations, protocol 1. Annealing simulations were then performed using protocol 3 in order to preserve the spacing between cellulose layers.

Table 2. Constants used to calculate the fugacity constant (for pressure in bar and temperature in K) in the virial equation of state developed by Spycher and Reed.[72]

Constant	Value
a	-12.6
b	2.60×10^{-1}
c	-7.25×10^{-5}
d	4.72×10^{-3}
e	-2.70×10^{-5}
f	2.16×10^{-8}

2.4. Hydrogen Sorption

Sorption simulations were performed in the Grand Canonical (GC) Ensemble using DL_MONTE with Metropolis algorithm acceptance probabilities. Hydrogen molecules were modelled using the Lennard-Jones interactions from Yang and Zhong [71] with cross terms between hydrogen and cellulose generated according to Lorentz-Berthelot mixing rules. 1,000,000 moves were performed, 50,000 of which were equilibrium, with 20% translations, 20% rotations and 60% insertions/removals. Adsorption isotherms were generated at 298 K for partial pressures in the range $1-10^3$ atm. In all calculations the substrate atoms were fixed. Example input files are provided in the data repository. The chemical activity of hydrogen molecules changes as a function of partial pressure. Assuming ideal gas behaviour

$$\mu = \mu_0 + RT \ln \frac{P}{P_0}, \tag{1}$$

where μ is the chemical potential, μ_0 a reference potential, R the molar gas constant, T temperature with P and P_0 the partial and reference pressures respectively. At high partial pressure, the ideal behaviour begins to break down. This deviation from ideal behaviour is expressed by the fugacity calculated according to the equation of state derived by Spycher and Reed [72],

$$\ln \varphi = ((\frac{a}{T^2} + \frac{b}{T} + c)P + \frac{d}{T^2} + \frac{e}{T} + f)P^2)/2, \tag{2}$$

where φ is the fugacity constant, T is the temperature, P is the partial pressure, and $a - f$ are constants which for hydrogren take the values given in Table 2.4. The fugacity, F is then calculated according to

$$F = \varphi \times P. \tag{3}$$

The DL_MONTE input files specify the partial pressure, from which chemical activity is determined according to Equation 1. In our data and plots we correct this to the fugacity, as per Equations 2 and 3, to account for departure from ideal behaviour at high pressures.

2.5. Hydrogen Diffusion

In order for sorption and desorption to occur readily, it is not sufficient for the adsorbate to be able to fit in a given structure, it must also be capable of diffusing through it. Hence following each GCMC simulation, the final structures from these sorption calculations were returned to DL_POLY to model the diffusion of hydrogen molecules in the different structures at a range of hydrogen densities, using protocol 4. The behaviour of hydrogen molecules within slit pore, amorphous and pinned cellulose structures was investigated, at high, medium and low partial pressures. The frameworks were held rigid throughout simulations of slit pore and pinned cellulose structures, whereas the amorphous structures were not fixed. The behaviour was characterised by the mean squared displacement (MSD) which measures the average displacement of atoms in the system over a period of time, given by

$$MSD = <|r(t) - r(0)|^2>, \tag{4}$$

where $r(t)$ is the position at time t.

2.6. Hydrogen Sorption Sites

The positions of the hydrogen sorption sites within the cellulose framework were calculated from a density map with a bin size of 0.1 Å. The number of hydrogen molecules at given positions during GCMC calculations was calculated from the DL_MONTE output. The generated maps of hydrogen position were superimposed on the empty cellulose configurations which were the initial inputs for the GCMC calculations.

3. Results

3.1. Structure Stability

The first step was to confirm the stability of the Iβ allomorph of cellulose generated by cellulose-builder and that the potential model had been correctly determined and assigned by DL_FIELD. To this end molecular dynamics simulations were performed with protocol 4 and the results are summarised in Table 3.

Table 3. Changes to density and cell parameters during simulation of crystalline Iβ cellulose of different chain lengths (DP)

Chain length	Initial Density(g cm^{-3})	Δa(%)	Δb(%)	Δc(%)	Δvolume(%)	Final Density(g cm^{-3})
2	1.69	4.2	2.9	6.8	10.7	1.53
3	1.67	2.8	1.7	4.9	7.6	1.55
4	1.66	1.6	1.8	4.4	7.2	1.55
6	1.65	1.0	1.3	3.2	4.2	1.58
8	1.65	0.8	1.6	2.4	4.4	1.58
12	1.64	0.9	1.3	1.7	3.4	1.59

During relaxation, the unit cell parameters changed by less than 7% and the total volume of the cell changed by less than 11% however these changes are most prominent

with the shortest chains. It is important to bear in mind the polymeric nature of cellulose in practice and the clear trend observed. The experimental crystalline density of the Iβ allomorph of cellulose is is 1.63 g cm^{-3} as determined from the results of Nishiyama et al [66,73].These findings were for chains with a DP >12. [48,66]

The crystalline density of unrelaxed structures produced directly from cellulose-builder differed from this value by less than 4% and this reduces with increasing DP. In contrast the density of relaxed structures increases with DP to approach the experimental value. This is likely because the ends of the cellulose are tightly packed in the crystalline form generated by cellulose-builder but when allowed to relax the system expand to accommodate them and their motion. Overall the small changes in volume indicate that the crystalline Iβ allomorph is stable and OPLS_2005 force field is correctly implemented for cellulose by DL_FIELD. A degree of polymerisation of six (DP = 6) was chosen for all cellulose chains in further simulations, as it represents a compromise between approximating the experimental density and reasonable simulation size.

3.2. Hydrogen Sorption

Gas storage within a system is driven by two distinct phenomena: sorption and steric containment. Sorption occurs when there is significant interaction between the framework and the absorbing species, whereas, steric containment occurs when there is sufficient free space for a species to fit. To capture both aspects of storage, hydrogen storage within the modelled systems is presented as a function of volumetric density - mass of hydrogen per unit volume, as opposed to mass of hydrogen per mass of cellulose. As inter-sheet separation increases, the mass of cellulose within a given volume decreases and as a result is driven by steric storage, thus we will also make comparison with the pure hydrogen model 'in vacuum' i.e. with no substrate present. Calculations with the pure cellulose crystal resulted in no hydrogen sorption. This can be understood by considering van der Waals interactions between the hydrogen and the cellulose.

The cross terms derived for molecular hydrogen-cellulose carbon Lennard-Jones interactions have a radius of σ = 3.11 Å and the layer spacing in the crystalline Iβ structure is 3.76 Å meaning that there is insufficient space in the pure structure. In order to examine the sorptive properties of cellulose, we therefore turned to slit pore structures with increasing separation between layers. Isotherms of the volumetric density of hydrogen molecules within slit pore structures with a range of inter-layer spacings as a function of pressure are plotted in Fig. 3. The density of hydrogen molecules within an empty simulation cell are also shown.

These calculations show that the storage capacity of the slit pore cellulose structures increased with increasing inter-sheet separation. At simulated fugacities of less than approximately 300 bar, hydrogen densities of systems containing cellulose are greater than empty systems, which indicates preferential sorption to the cellulose structure. Therefore throughout the simulations, the cellulose framework promotes hydrogen storage at these fugacities. At simulated fugacities above 300 bar, greater densities of hydrogen could be stored in an empty vessel. This cross-over point exists as the cellulose framework itself occupies volume which could potentially store hydrogen molecules and at high pressures, steric containment outweighs the benefits of sorption.[74] We also note that at the highest pressures considered the density of hydrogen begins to approach its liquid density 74 kg m^{-3} at which point we expect the potential model

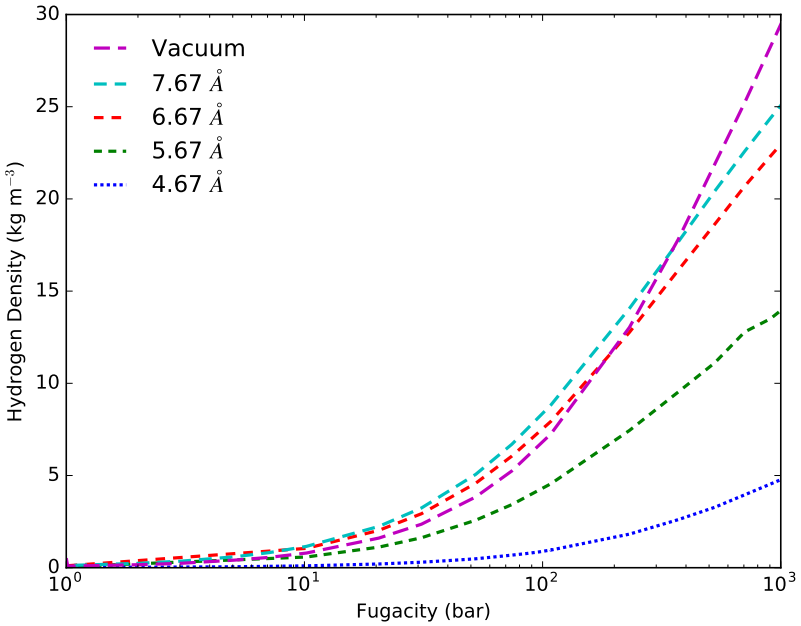

Figure 3. Isotherms for simulated hydrogen molecule adsorption within various cellulose slit pore structures at 298 K.

Table 4. Hydrogen density (kg m^{-3}) as a function of fugacity for slit pore, pinned and amorphous structures.

	Slit pore		Pinned		Amorphous	
Fugacity (bar)	Narrow	Wide	Narrow	Wide	Narrow	Wide
10.2	0.10	1.2	0.00	0.9	0.01	0.20
108	0.96	8.8	0.01	7.1	0.13	1.6
1960	6.4	29	0.07	26	0.87	6.3

to breakdown.

Two inter-sheet separations, 4.67 and 7.67 Å, were selected for further study as they represent the smallest inter-sheet separation found to be capable of significant hydrogen storage and the largest enhanced sorption over vacuum, respectively. We refer to the structures as narrow slit pore and wide slit pore throughout. Amorphous and pinned structures were annealed from each of the crystalline systems, to give narrow amorphous, wide amorphous, narrow pinned and wide pinned structures, respectively. As would be expected the larger spacing between sheets consistently increased the density of hydrogen adsorbed. As would be expected the larger spacing between sheets consistently increased the density of hydrogen adsorbed (Table 4). The amorphous systems were typically found to hold very little hydrogen suggesting that the relaxation had removed the majority of pores from the systems. Interesting behaviour was observed in the pinned structures however, where in the wide slit pore structure displayed similar sorption when compared with the pure crystalline structures. This is in contrast to the narrow slit pore structure where no sorption was observed in the pinned structure.

3.3. Hydrogen Diffusion

We now turn to characterising the diffusive behaviour of absorbed hydrogen, showing data for the unrelaxed slit pore structures in Fig. 4. In the narrow slit pore the MSD reaches $\sim 1.1\text{Å}^2$ but then plateaus, indicating that the molecule is trapped in a pore for at least the accessible timescales. The small MSD is indicative of a rattling, during which the molecule fully explores the pore. In contrast the wide slit pore structures show an MSD which rises to $\sim 1600\text{Å}^2$ indicating that hydrogen in these structures is mobile. The MSD is linear in time which also suggests that the motion is diffusive in character.

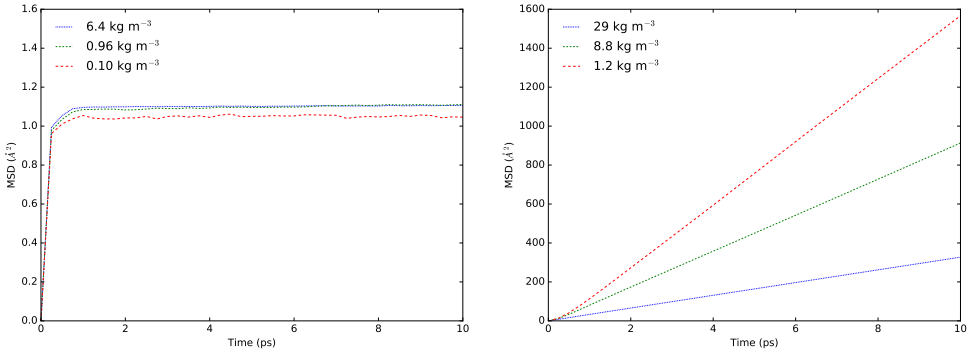

Figure 4. Simulated mean squared displacement of hydrogen molecules within narrow (left) and wide (right) slit pore structures. In narrow slit pores limited movement is observed, consistent with rattling motion of hydrogen trapped in pores. In wider pores more typical diffusive behaviour indicates that hydrogen is able to diffuse through the structure.

We can in turn break the MSD into components aligned with the x, y and z directions (approximately the a, b and c lattice vectors in Fig. 2). This decomposition is shown in Fig. 5. In the narrow slit pore, the MSD in each direction was similar, but increasing from x to z to y, indicating that the extent of mobility is least perpendicular to sheets and most parallel to chains. In wide slit pore structures, however, the diffusion is found to be highly directional and parallel to the cellulose sheets, the component in the x direction does not move from 0 at this scale.

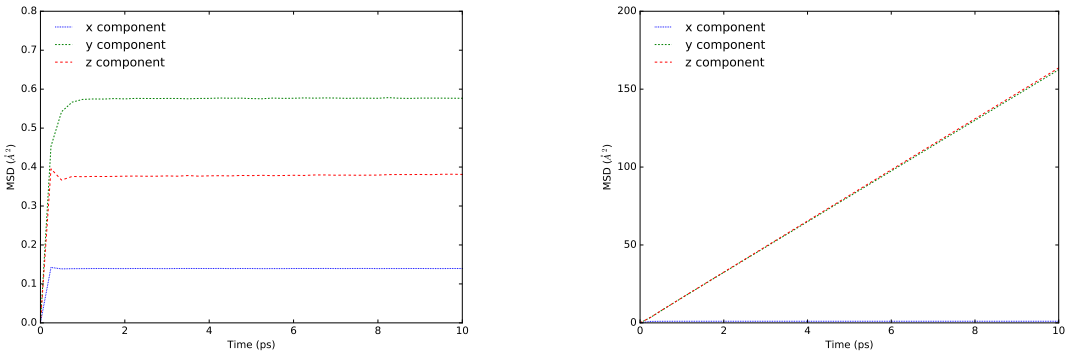

Figure 5. Simulated mean squared displacement of hydrogen molecules within narrow and wide cellulose structures with slit porosity, decomposed into the x,y and z components.

In Fig. 6 we show the MSD of hydrogen molecules in the amorphous structures. In the narrow systems at low density the behaviour is similar for the previous slit pore

structure. At low density and in the wide structure we see intermediate behaviour, with MSD neither plateauing nor reaching a linear limit. This suggests that a number of timescales may be involved and indeed, visualisations of trajectories suggested that relative movement of cellulose may be occurring on these timescales which will in turn activate motion of hydrogen. The observation is a reflection of the decreased order within the systems compared to slit pore structures but longer simulations are required to investigate this behaviour fully. Finally we considered the pinned structures in Fig. 7, where behaviour is consistent with the slit pore structures though mobility is reduced due to the reduced order of the substrate.

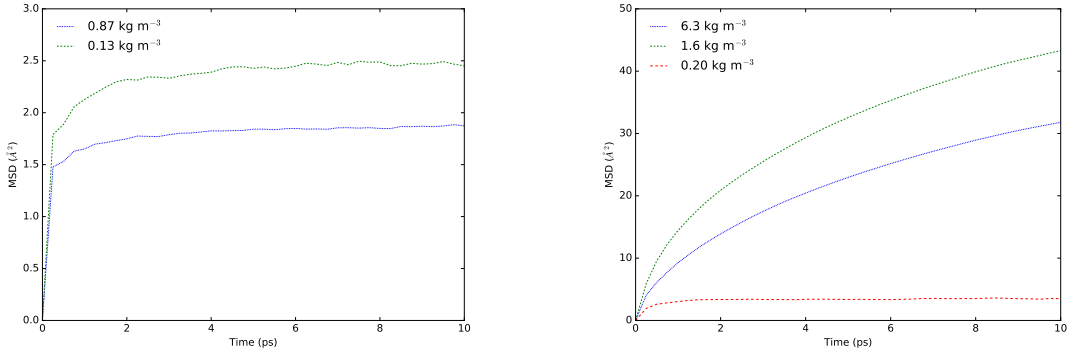

Figure 6. Simulated mean squared displacement of hydrogen molecules within (left) narrow and (right) wide amorphous structures. In narrow structures contrasting behaviour is seen with motion consistent with rattling at low density, with increased mobility in the higher density systems. Similar behaviour is also seen in the wide structures, indicative of activated diffusion on two or more timescales.

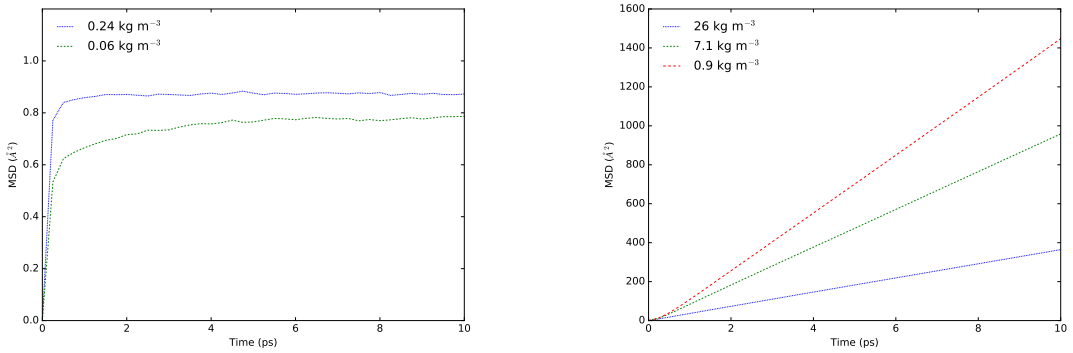

Figure 7. Mean squared displacement of hydrogen in (left) narrow and (right) wide pinned structures. Mobility is reduced but behaviour is consistent with the slit pore structures with rattling motion in narrow and diffusion in wide structures.

3.4. Hydrogen Sorption Sites

Finally, we will discuss the location of the hydrogen sorption sites within wide and narrow slit pore structures, shown in Figures 8 and 9 (these and Fig. 10 were generated with VESTA [75]). Hydrogen molecules within narrow slit pore structures are found in discrete and localised positions. The hydrogen molecules are trapped in the voids by the hydroxymethyl groups and linking oxygens between sheets of cellulose chains. In contrast, in wide slit pore structures hydrogen molecules occupy delocalised positions

between the sheets of cellulose chains.

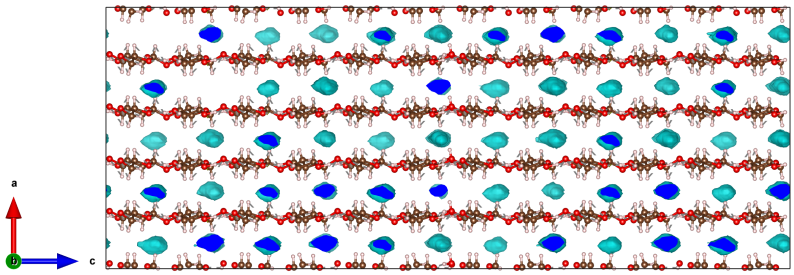

Figure 8. Visualised positions of sorption sites for hydrogen molecules within narrow slit pore structures.

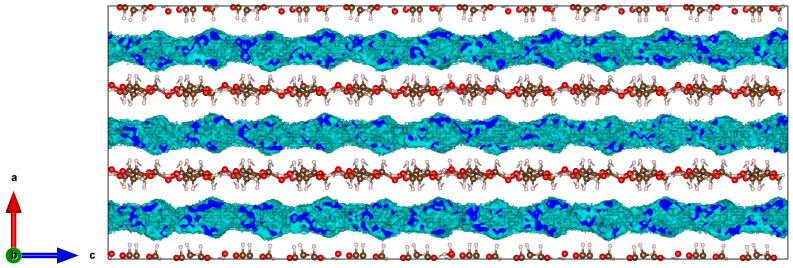

Figure 9. Visualised positions of sorption sites for hydrogen molecules within wide slit pore structures.

4. Conclusions

We have used codes in the DL_SOFTWARE suite, DL_POLY , DL_MONTE with DL_FIELD to perform hydrogen sorption and transport studies in a range of cellulose frameworks. The common interfaces of these codes is valuable in allowing the use of the appropriate simulation method at each stage of our calculations. This work has shown that cellulose demonstrates hydrogen storage potential at experimentally accessible pressures (<100 bar).

No hydrogen sorption was observed in pure crystalline cellulose. Simulations of some slit pore model structures that below fugacities of 300 bar, cellulose shows higher hydrogen density than is observed in vacuum, indicating that the cellulose structure and pore size influences the hydrogen storage capacity. The most suitable candidate for hydrogen storage density was observed in wide pinned structures (with initial spacing

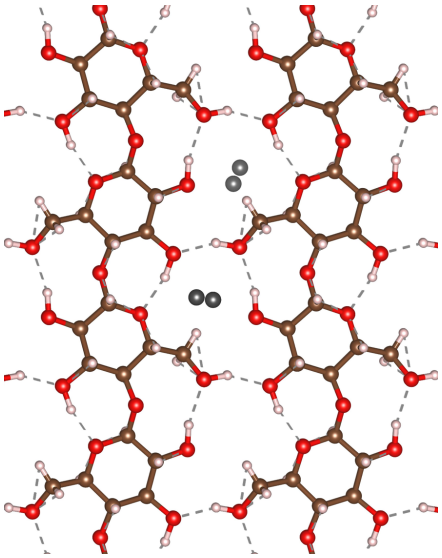

Figure 10. Visualised positions of hydrogen molecules (grey) within narrow slit pore structures.

7.67 Å), having a capacity of 7.1 kg m^{-3} at 100 bar, where we also observed that hydrogen had reasonable mobility indicating that sorption and desorption of hydrogen from the structures should be possible.

While our work demonstrates that cellulose shows potential as a hydrogen storage material at reasonable pressures it seems likely that native cellulose does not contain sufficient porosity to facilitate significant storage. Further work is therefore required to evaluate whether our slit pore model systems might be able to reproduce more complex amorphous porous cellulose based structures. Simulations of amorphous structures and experiment would then help to understand whether these structures have the capacity and the mobility necessary for use in hydrogen storage. This work should also compare other biomolecular and hydrogen forcefields, including the use of Feynmann-Hibbs corrections where appropriate since this will confirm the robustness of our results.

Data availability

The data supporting the findings of this study are openly available at `https://doi.org/10.5281/zenodo.2538053`.

Acknowledgement(s)

This research made use of the Balena High Performance Computing Service at the University of Bath and used the Isambard UK National Tier-2 HPC Service (`http://gw4.ac.uk/isambard/`) operated by GW4 and the UK Met Office, and funded by EPSRC (EP/P020224/1).

Funding

MRS and LOY acknowledge funding from the EPSRC for a Ph.D. studentship funding through the EPSRC Centre for Doctorial Training in Sustainable Chemical Technologies, University of Bath (EP/L016354/1). CY acknowledges the CCP5 funding and associated CoSeC support at STFC via EPSRC grant no: EP/M022617/1. TJM acknowledges funding via EPRSC grant nos: EP/K021109/1, EP/L018365/1 and EP/P024807/1.

References

[1] Parmesan C, Yohe G. A globally coherent fingerprint of climate change impacts across natural systems. Nature. 2003;421(6918):37–42. Available from: http://www.ncbi.nlm.nih.gov/pubmed/12511946.

[2] Schuth F. Chemical Compounds for Energy Storage. Chemie Ingenieur Technik. 2011; 83(11):1984–1993.

[3] Eberle U, Felderhoff M, Schüth F. Chemical and physical solutions for hydrogen storage. Angewandte Chemie - International Edition. 2009;48(36):6608–6630.

[4] Müller K, Arlt W. Status and Development in Hydrogen Transport and Storage for Energy Applications. Energy Technology. 2013;1(9):501–511. Available from: http://dx.doi.org/10.1002/ente.201300055.

[5] McKeown NB, Budd PM, Book D. Microporous polymers as potential hydrogen storage materials. Macromolecular Rapid Communications. 2007;28(9):995–1002.

[6] Germain J, Frechet JMJ, Svec F. Nanoporous polymers for hydrogen storage. Small. 2009; 5(10):1098–1111.

[7] Mandal TK, Gregory DH. Hydrogen: A future energy vector for sustainable development. Proceedings of the Institution of Mechanical Engineers, Part C: Journal of Mechanical Engineering Science. 2010;224(3):539–558. Available from: http://www.scopus.com/inward/record.url?eid=2-s2.0-77949700512{&}partnerID=40{&}md5=e566722e62431a649a6d1db5801701f2.

[8] Liu C, Li F, Ma LP, et al. Advanced Materials for Energy Storage. Advanced Materials. 2010;22(8):E28–E62. Available from: http://doi.wiley.com/10.1002/adma.200903328.

[9] Schlapbach L, Züttel A. Hydrogen-storage materials for mobile applications. Nature. 2001;414(6861):353–358. Available from: http://www.nature.com/doifinder/10.1038/35104634.

[10] Düren T, Bae YS, Snurr RQ. Using molecular simulation to characterise metal-organic frameworks for adsorption applications. Chemical Society Reviews. 2009;38(5):1237. Available from: http://xlink.rsc.org/?DOI=b803498m.

[11] Pukazhselvan D, Kumar V, Singh SK. High capacity hydrogen storage: Basic aspects, new developments and milestones. Nano Energy. 2012;1(4):566–589. Available from: http://dx.doi.org/10.1016/j.nanoen.2012.05.004.

[12] Fairen-Jimenez D, Moggach SA, Wharmby MT, et al. Opening the gate: Framework flexibility in ZIF-8 explored by experiments and simulations. Journal of the American Chemical Society. 2011;133(23):8900–8902.

[13] Trewin A, Willock DJ, Cooper AI. Atomistic Simulation of Micropore Structure , Surface Area , and Gas Sorption Properties for Amorphous Microporous Polymer Networks. Journal of Physical Chemistry. 2008;1112:20549–20559.

[14] McKeown NB, Budd PM. Polymers of intrinsic microporosity (PIMs): organic materials for membrane separations, heterogeneous catalysis and hydrogen storage. Chemical Society Reviews. 2006;35(8):675. Available from: http://xlink.rsc.org/?DOI=b600349d.

[15] Lauren J Abbott and Coray M Colina. Atomistic structure generation and gas adsorption

simulations of microporous polymer networks. Macromolecules. 2011;44(11):4511–4519.
[16] Dawson R, Cooper AI, Adams DJ. Nanoporous organic polymer networks. Progress in Polymer Science. 2012;37(4):530–563. Available from: http://dx.doi.org/10.1016/j.progpolymsci.2011.09.002.
[17] Larsen GS, Lin P, Siperstein FR, et al. Methane adsorption in PIM-1. Adsorption. 2011; 17(1):21–26.
[18] Madkour TM, Mark JE. Molecular modeling investigation of the fundamental structural parameters of polymers of intrinsic microporosity for the design of tailor-made ultrapermeable and highly selective gas separation membranes. Journal of Membrane Science. 2013;431:37–46. Available from: http://dx.doi.org/10.1016/j.memsci.2012.12.033.
[19] Minelli M, Friess K, Vopička O, et al. Modeling gas and vapor sorption in a polymer of intrinsic microporosity (PIM-1). Fluid Phase Equilibria. 2013;347:35–44.
[20] Heuchel M, Fritsch D, Budd PM, et al. Atomistic packing model and free volume distribution of a polymer with intrinsic microporosity (PIM-1). Journal of Membrane Science. 2008;318(1-2):84–99.
[21] Wood CD, Tan B, Trewin A, et al. Hydrogen Storage in Microporous\nHypercrosslinked Organic Polymer Networks. Chemistry of Materials. 2007;19(8):2034–2048.
[22] Jiang S, Jelfs KE, Holden D, et al. Molecular dynamics simulations of gas selectivity in amorphous porous molecular solids. Journal of the American Chemical Society. 2013; 135(47):17818–17830.
[23] Medronho B, Romano A, Miguel MG, et al. Rationalizing cellulose (in)solubility: Reviewing basic physicochemical aspects and role of hydrophobic interactions. Cellulose. 2012; 19(3):581–587.
[24] Krishnamachari P, Hashaikeh R, Tiner M. Modified cellulose morphologies and its composites; SEM and TEM analysis. Micron. 2011;42(8):751–761.
[25] Pérez S, Samain D. Structure and Engineering of Celluloses. Advances in Carbohydrate Chemistry and Biochemistry. 2010;64(C):26–116.
[26] Rahimi M, Behrooz R. Effect of Cellulose Characteristic and Hydrolyze Conditions on Morphology and Size of Nanocrystal Cellulose Extracted from Wheat Straw. International Journal of Polymeric Materials. 2011;60(8):529–541.
[27] Oehme DP, Downton MT, Doblin MS, et al. Unique aspects of the structure and dynamics of elementary iβ cellulose microfibrils revealed by computational simulations. Plant physiology. 2015;168(1):3–17. Available from: http://www.plantphysiol.org/content/168/1/3.abstract.
[28] Brown RM, Saxena IM. Cellulose biosynthesis: A model for understanding the assembly of biopolymers. Plant Physiology and Biochemistry. 2000;38(1-2):57–67.
[29] Matthews JF, Skopec CE, Mason PE, et al. Computer simulation studies of microcrystalline cellulose Iβ. Carbohydrate Research. 2006;341(1):138–152.
[30] Klemm D, Heublein B, Fink HP, et al. Cellulose: Fascinating biopolymer and sustainable raw material. Angewandte Chemie - International Edition. 2005;44(22):3358–3393.
[31] Atalla RH. The Structures of Cellulose. Materials Research Society Proceedings. 1990; 197:89–98.
[32] Ding SY, Himmel ME. The maize primary cell wall microfibril: a new model derived from direct visualization. Agricultural and Food Chemistry. 2006;54(3):597–606. Available from: http://www.ncbi.nlm.nih.gov/pubmed/16448156.
[33] Ciolacu D, Ciolacu F, Popa VI. Supramolecular structure - A key parameter for cellulose biodegradation. Macromolecular Symposia. 2008;272(1):136–142.
[34] Nishiyama Y, Sugiyama J, Chanzy H, et al. Crystal structure and hydrogen bonding system in cellulose I(alpha) from synchrotron X-ray and neutron fiber diffraction. Journal of the American Chemical Society. 2003;125(47):14300–14306.
[35] Cosgrove DJ. Growth of the plant cell wall. Nature reviews Molecular cell biology. 2005; 6(November):850–861.
[36] Namboori K, Ramachandran KI, Deepa G. Computational Chemistry and Molecular Modeling. ; 2008. Available from: http://link.springer.com/10.1007/

978-3-540-77304-7.

[37] Damm W, Frontera A, Tirado-Rives J, et al. OPLS all-atom force field for carbohydrates. Journal of Computational Chemistry. 1997;18(16):1955–1970. Available from: http://dx.doi.org/10.1002/(SICI)1096-987X(199712)18:16{%}3C1955::AID-JCC1{%}3E3.0.CO;2-L{%}5Cnhttp://onlinelibrary.wiley.com/store/10.1002/(SICI)1096-987X(199712)18:16{%}3C1955::AID-JCC1{%}3E3.0.CO;2-L/asset/1{_}ftp.pdf?v=1{&}t=h1romdba{&}s=52e376183e639ea82e4cf13d732c41.

[38] Miyamoto H, Yamane C, Ueda K. Molecular dynamics simulation of dehydration in cellulose/water crystals. Cellulose. 2015;22(5):2899–2910.

[39] Miyamoto H, Schnupf U, Crowley MF, et al. Comparison of the simulations of cellulosic crystals with three carbohydrate force fields. Carbohydrate Research. 2016;422:17–23. Available from: http://dx.doi.org/10.1016/j.carres.2016.01.001.

[40] Guvench O, Mallajosyula SS, Raman EP, et al. CHARMM Additive All-Atom Force Field for Carbohydrate Derivatives and Its Utility in Polysaccharide and CarbohydrateProtein Modeling. Journal of Chemical Theory and Computation. 2011 oct;7(10):3162–3180. Available from: http://pubs.acs.org/doi/abs/10.1021/ct200328phttp://www.ncbi.nlm.nih.gov/pubmed/22125473http://www.pubmedcentral.nih.gov/articlerender.fcgi?artid=PMC3224046.

[41] Momany FA, Willett J, Schnupf U. Molecular dynamics simulations of a cyclic-DP-240 amylose fragment in a periodic cell: Glass transition temperature and water diffusion. Carbohydrate Polymers. 2009 nov;78(4):978–986. Available from: https://doi.org/10.1016/j.carbpol.2009.07.034http://linkinghub.elsevier.com/retrieve/pii/S0144861709003981.

[42] Banks JL, Beard HS, Cao Y, et al. Integrated Modeling Program, Applied Chemical Theory (IMPACT). Journal of Computational Chemistry. 2005 dec;26(16):1752–1780. Available from: http://doi.wiley.com/10.1002/jcc.20292.

[43] Hadden JA, French AD, Woods RJ. Unraveling cellulose microfibrils: A twisted tale. Biopolymers. 2013;99(10):746–756.

[44] Bergenstråhle M, Wohlert J, Larsson PT, et al. Dynamics of cellulose-water interfaces: NMR spin-lattice relaxation times calculated from atomistic computer simulations. The journal of physical chemistry B. 2008;112(9):2590–2595.

[45] Liao R, Zhu M, Zhou XIN, et al. Molecular Dynamics Study of the Disruption of H-BONDS by Water Molecules and its Diffusion Behavior in Amorphous Cellulose. Modern Physics Letters B. 2012;26(14):1–14.

[46] Kulasinski K, Keten S, Churakov SV, et al. A comparative molecular dynamics study of crystalline, paracrystalline and amorphous states of cellulose. Cellulose. 2014;21(3):1103–1116.

[47] Tanaka F, Iwata T. Estimation of the elastic modulus of cellulose crystal by molecular mechanics simulation. Cellulose. 2006;13(5):509–517.

[48] Djahedi C, Berglund LA, Wohlert J. Molecular deformation mechanisms in cellulose allomorphs and the role of hydrogen bonds. Carbohydrate Polymers. 2015;130:175–182. Available from: http://dx.doi.org/10.1016/j.carbpol.2015.04.073.

[49] Bergenstråhle M, Berglund LA, Mazeau K. Thermal response in crystalline Ibeta cellulose: a molecular dynamics study. The Journal of Physical Chemistry B. 2007;111(30):9138–9145.

[50] Chen P, Nishiyama Y, Mazeau K. Torsional Entropy at the Origin of the Reversible Temperature- Induced Phase Transition of Cellulose. Macromolecules. 2012;45(1):362–368.

[51] Chen W, Lickfield GC, Yang CQ. Molecular modeling of cellulose in amorphous state. Part I: Model building and plastic deformation study. Polymer. 2004;45(3):1063–1071.

[52] Wohlert J, Bergenstråhle-Wohlert M, Berglund LA. Deformation of cellulose nanocrystals: Entropy, internal energy and temperature dependence. Cellulose. 2012;19(6):1821–1836.

[53] Bazooyar F, Taherzadeh M, Niklasson C, et al. Molecular modelling of cellulose dissolution. Journal of Computational and Theoretical Nanoscience. 2013;10(11):2639–2646.

[54] Glasser WG, Atalla RH, Blackwell J, et al. About the structure of cellulose : debating the Lindman hypothesis. Molecular Biosciences. 2012;:589–598.
[55] Heiner AP, Kuutti L, Teleman O. Comparison of the interface between water and four surfaces of native crystalline cellulose by molecular dynamics simulations. Carbohydrate Research. 1998;306(1-2):205–220.
[56] Li L, Pérré P, Frank X, et al. A coarse-grain force-field for xylan and its interaction with cellulose. Carbohydrate Polymers. 2015;127:438–450.
[57] Mazeau K, Wyszomirski M. Modelling of Congo red adsorption on the hydrophobic surface of cellulose using molecular dynamics. Cellulose. 2012;19(5):1495–1506.
[58] Woodcock S, Henrissat B, Sugiyama J. Docking of Congo Red to the surface of crystalline cellulose using molecular mechanics. Biopolymers. 1995;36(2):201–210.
[59] Da Silva Perez D, Ruggiero R, Morais LC, et al. Theoretical and experimental studies on the adsorption of aromatic compounds onto cellulose. Langmuir : the ACS journal of surfaces and colloids. 2004;20(8):3151–3158.
[60] Todorov I, Smith W. DL_POLY_3: The CCP5 National UK Code for Molecular-Dynamics Simulations. Philosophical Transactions: Mathematical, Physical and Engineering Sciences. 2004;362(1822):1835–1852. Available from: http://www.jstor.org/stable/4142464.
[61] Todorov IT, Smith W, Trachenko K, et al. DL_POLY_3: new dimensions in molecular dynamics simulations via massive parallelism. Journal of Materials Chemistry. 2006; 16(20):1911. Available from: http://xlink.rsc.org/?DOI=b517931a.
[62] Purton J, Crabtree J, Parker S. DL_MONTE: A general purpose program for parallel Monte Carlo simulation. Molecular Simulation. 2013;39:1240–1252.
[63] Brukhno A, Grant J, Underwood TL, et al. DL MONTE: A multipurpose code for Monte Carlo simulation. arXiv. 2018;1803.00484.
[64] Yong C. Descriptions and Implementations of DL_F Notation: A Natural Chemical Expression System of Atom Types for Molecular Simulations. The Journal of Chemical Information and Modeling. 2016;56(8):1405–1409.
[65] Gomes TCF, Skaf MS. Cellulose-builder: A toolkit for building crystalline structures of cellulose. Journal of Computational Chemistry. 2012;33(14):1338–1346.
[66] Nishiyama Y, Sugiyama J, Chanzy H, et al. Crystal structure and hydrogen bonding system in cellulose Iα from synchrotron x-ray and neutron fiber diffraction. Journal of the American Chemical Society. 2003;125(47):14300–14306. Available from: http://www.ncbi.nlm.nih.gov/entrez/query.fcgi?db=pubmed{&}cmd=Retrieve{&}dopt=AbstractPlus{&}list{_}uids=3737771244308919 71related:w8tIt31A3zMJ.
[67] Park S, Venditti RA, Jameel H, et al. Changes in pore size distribution during the drying of cellulose fibers as measured by differential scanning calorimetry. Carbohydrate Polymers. 2006;66(1):97–103.
[68] Guo C, Zhou L, Lv J. Effects of expandable graphite and modified ammonium polyphosphate on the flame-retardant and mechanical properties of wood flour-polypropylene composites. Polymers and Polymer Composites. 2013;21(7):449–456.
[69] Jorgensen WL, Maxwell DS, Tirado-Rives J. Development and Testing of the OLPS All-Atom Force Field on Conformational Energetics and Properties of Organic Liquids. Journal of the American Chemical Society. 1996;118(15):11225–11236. Available from: http://dx.doi.org/10.1021/ja9621760.
[70] Kony D, Damm W, Stoll S, et al. An improved OPLS-AA force field for carbohydrates. Journal of Computational Chemistry. 2002;23(15):1416–1429.
[71] Yang Q, Zhong C. Molecular simulation of adsorption and diffusion of hydrogen in metal-organic frameworks. Journal of Physical Chemistry B. 2005;109(24):11862–11864.
[72] Spycher NF, Reed MH. Fugacity coefficients of H2, CO2, CH4, H2O and of H2O- CO2-CH4 mixtures: A virial equation treatment for moderate pressures and temperatures applicable to calculations of hydrothermal boiling. Geochimica et Cosmochimica Acta. 1988;52(3):739–749.
[73] Zhang Q, Bulone V, Agren H, et al. A molecular dynamics study of the thermal response

of crystalline cellulose I?? Cellulose. 2011;18(2):207–221.

[74] Bimbo N, Ting VP, Sharpe JE, et al. Analysis of optimal conditions for adsorptive hydrogen storage in microporous solids. Colloids and Surfaces A: Physicochemical and Engineering Aspects. 2013;437:113–119. Available from: http://dx.doi.org/10.1016/j.colsurfa.2012.11.008.

[75] Momma K, Izumi F. *VESTA3* for three-dimensional visualization of crystal, volumetric and morphology data. Journal of Applied Crystallography. 2011 Dec;44(6):1272–1276. Available from: https://doi.org/10.1107/S0021889811038970.